APPLIED GEOPHYSICS, Vol.12, No.1 (March 2015), P. 1-10, 7 Figures.
DOI: 10.1007/s11770-014-0477-1

Effect of pore structure on seismic rock-physics characteristics of dense carbonates*

Pan Jian-Guo[1], Wang Hong-Bin[1], Li Chuang[1], and Zhao Jian-Guo♦[2]

Abstract: The Ordovician carbonate rocks of the Yingshan formation in the Tarim Basin have a complex pore structure owing to diagenetic and secondary structures. Seismic elastic parameters (e.g., wave velocity) depend on porosity and pore structure. We estimated the average specific surface, average pore-throat radius, pore roundness, and average aspect ratio of carbonate rocks from the Tazhong area. High P-wave velocity samples have small average specific surface, small average pore-throat radius, and large average aspect ratio. Differences in the pore structure of dense carbonate samples lead to fluid-related velocity variability. However, the relation between velocity dispersion and average specific surface, or the average aspect ratio, is not linear. For large or small average specific surface, the pore structure of the rock samples becomes uniform, which weakens squirt flow and minimizes the residuals of ultrasonic data and predictions with the Gassmann equation. When rigid dissolved (casting mold) pores coexist with less rigid microcracks, there are significant P-wave velocity differences between measurements and predictions.
Keywords: Carbonate rocks, pore structure, elastic parameters, microstructure, Tarim Basin

Introduction

The Ordovician marine carbonate reservoir in Tarim Basin is important to the onshore oil and gas exploration in China. Oil and gas exploration in this horizon has progressed from the exploration of large bead-like oil and gas reservoirs by using seismic methods to the exploration of widely distributed small reservoirs, which requires more accurate imaging techniques and greater emphasis on reservoir identification, hydrocarbon detection, and modeling of seismic rock physics.

There are many experimental and theoretical studies of the seismic rock physics of carbonate rocks. Ultrasonic velocity measurements and microstructure analysis have revealed that the diversity of pore types is the main reason for the velocity differences in carbonates (Anselmetti and Eberli, 1993, 1999). For instance, ultrasonic velocity exceeds 2500 m/s in carbonates with near-spherical molding pores (Baechle et al., 2007, 2008), and carbonates with different pore types exhibit velocity variability under dry and water-saturated conditions (Agersborg et al., 2008). Verwer et al. (2010) analyzed the interaction between porosity variability and the fluid and rock matrix in carbonates and the effect on dynamic shear modulus. They pointed

Manuscript received by the Editor December 22, 2014; revised manuscript received February 16, 2015.
*This work was supported by the Natural Science Foundation of China (No. 41274138).
1. Northwest Branch of PetroChina Exploration and Development Research Institute, Lanzhou 730020, China.
2. College of Geophysics and Information Engineering, China University of Petroleum, Beijing 102249, China.
♦Corresponding Author: Zhao Jian-Guo (Email: jgzhao761215@aliyun.com)

out that rock samples with large specific surface exhibit strong fluid–rock interaction and remarkable reduction in shear modulus. Sharma et al. (2013) used computed tomography (CT) to examine the sensitivity of flow and elastic properties to fabric heterogeneity in carbonates. Inclusions with different aspect ratios are used to characterize the different types of pores in carbonate rocks; furthermore, the self-consistent model (SCA) or differential equivalent model (DEM) are used to quantify the effect of porosity variation on the velocity and the elastic properties in carbonates with specific pore structure. For example, molds or vugs can be expressed as pores with large aspect ratio and thus have more contact boundaries than intergranular or intercrystalline pores. Consequently, the elastic modulus or velocity would increase at the same porosity. Xu and Payne (2009) classified the pores in carbonates into rigid pores, such as clay pores, intergranular pores, microcracks, and vugs, which are represented by ellipsoids with different aspect ratios, and characterized the relation between pore type and content and seismic elastic properties by using the DEM model. Liu et al. (2006) studied the acoustic parameters of Ordovician carbonate rocks from the Tahe oil field and the corresponding variation law. Zhou and Yang (2006) analyzed how fractures in carbonate rocks affect the rock elastic properties and velocity–porosity relation. Ba et al. (2011, 2013) developed a double porosity model for studying the factors affecting the seismic elastic properties in isotropic poroelastic media and obtained multiscale rock-physics templates for hydrocarbon detection in carbonate reservoirs. Nevertheless, studies regarding the seismic rock physics of low-porosity and low-permeability carbonate reservoirs are presently rare.

It is not difficult to infer from the abovementioned studies that pore types play a more important role than other factors, such as minerals and cement, in affecting the elastic properties, presumably, because carbonates have simpler mineralogy and more complex pore structure than sandstones. The pore structure of carbonates depends on the various stages of diagenesis. The carbonate rocks of the Ordovician Yingshan formation in the Tarim Basin are affected by normal compaction and chemical diagenesis, and post-tectonic events (e.g., structural fractures, weathering crust fractures, and leaching). Moreover, the pore structure of the carbonate reservoirs was strongly reworked, which resulted in a large variety of pore types. Diagenesis and secondary porosity formed rocks with complex porosity and structural characteristics, and the characteristics of low-porosity and low-permeability unconventional reservoirs. In this study, we analyzed the microstructures of Yingshan formation carbonate samples, conducted ultrasonic measurements, and we examined the effect of pore structure on the seismic elastic properties. This study can provide the basis for lithology identification and hydrocarbon detection in similar reservoirs.

Laboratory samples and microstructure characteristics

Fifty-nine carbonate samples from the Ordovician Yingshan formation were collected from nine wells in the Tazhong area. The carbonates were deposited in moderate- to high-energy banks and intraplatform shoals. The carbonate samples are a uniform sparry calcarenite with 0.20−1.50 mm sparry calcite grains and calcium carbonate content greater than 98%. The microscopic reservoir space mainly consists of pores and microcracks. Pores are intergranular dissolved pores, intragranular pores, casting pores, and other dissolution pores because of alternating hydrothermal activity in the late diagenetic and secondary dissolution stages. Hydrothermal activity also destroyed the original intergranular and intercrystalline pores. According to the CT imaging of the pore structure, the dissolved and casting pores are mainly spherical, or nearly spherical, with large pore aspect ratios. Statistical analysis shows that the aspect ratio of these pores varies between 0.1 and 0.9 and they constitute more than 80% of the pores. Microcracks are mainly attributed to tectonic activity during late diagenesis and most of them are half or fully filled with calcite; nevertheless, a small number of unfilled microcracks are observed. Based on the pore-filling characteristics, the observed cracks are not attributed to the release of stress during drilling or sampling. The presence of microcracks contributes little to the total porosity of the reservoir rocks but significantly affects the physical and elastic properties (e.g., permeability, velocity). The pore types of the collected samples fall into two groups. The first group comprises dissolved or casting pores, and the second group includes dissolved or casting pores and microcracks (Figure 1).

We made cast sheets of 41 carbonate rock samples. We then analyzed the 2D cast sheets to obtain the following pore-structure parameters. First, the parameter for describing the overall characteristics of the rock pore structure, such as the ratio of the total perimeter to the total area of pores in a given area, is the average specific surface (SS)—the ratio of superficial area to volume in

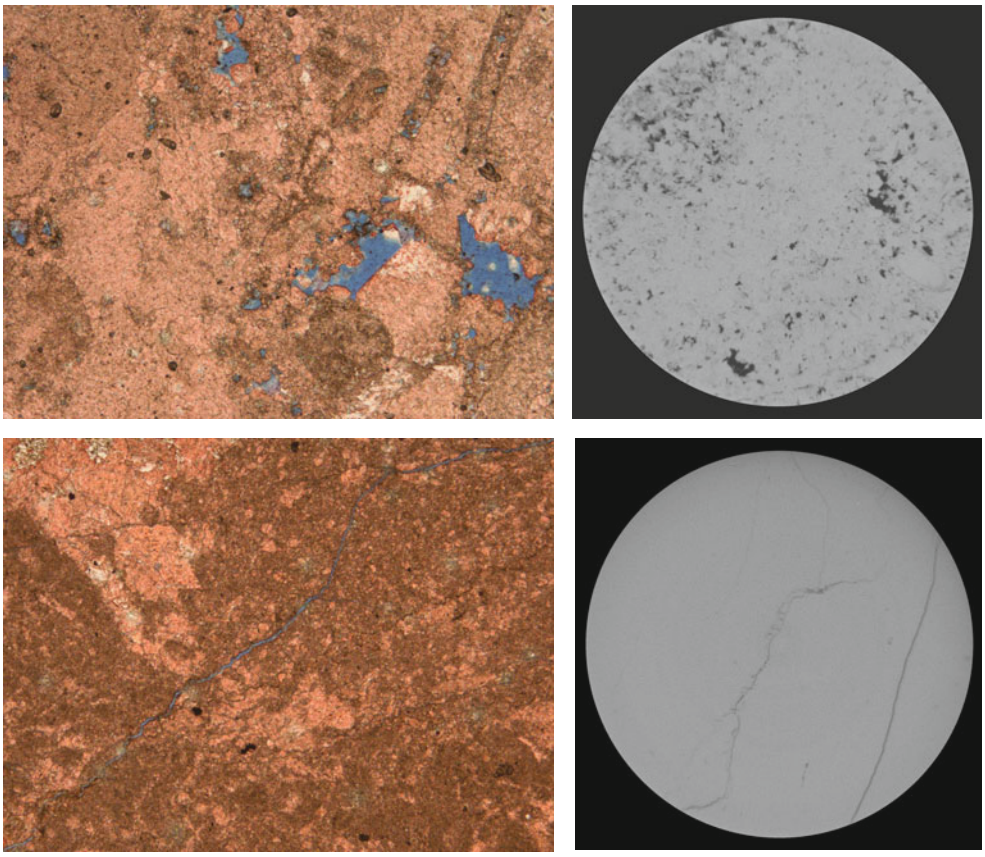

Fig.1 Microscopic pore structure of the carbonate samples.

a pore in three dimensions. A small SS indicates that the dissolved (casting) pores with large aspect ratio make up a higher percentage of the total pores in the rocks, whereas a high SS suggests that the cracks or dissolved (casting) pores with small aspect ratio are more. The average specific surface of the 41 samples is 17.4–239.9 mm^{-1}. The wide range of average specific surface also implies significant differences in the pore structure of the samples. Second, the parameter for describing the pores is the average pore-throat radius (R). The larger R is, the higher the pore connectivity is. From the point of view of elastic properties, the pore throat represents soft pores with small aspect ratio, such as microfractures, pore restriction zones, and grain contact boundaries. The larger the pore-throat radius is, pores are uniform and the double-pore structure is less abundant. The average pore-throat radius of the 41 samples is between 6.1 and 26.9 μm. Third, the parameters for describing the structural characteristics of the pores are the average pore roundness (γ) and aspect ratio (α). The average roundness of a pore refers to the degree to which the 2D cross section of a pore, except for the pore throat, is close to the theoretical roundness. The average aspect ratio refers to the average ratio of width to length of all pores including pore throats. The lower the average roundness and aspect ratio are, the closer the pore shape to flat cracks is; moreover, the pore rigidity is reduced. The average aspect ratio is between 0.02 and 0.14. The pore structure parameters of the samples are listed in Table 1.

Seismic rock-physics characteristics

In this study, we mainly focused on the acoustic characteristics of the rock samples under dry and water-saturated conditions. First, we washed the samples with toluene standard solution to remove the residual oil and salts in the pores and then dried the samples in an oven at 70 ˚C for 48 h. Thus, the samples are at relative dry conditions; that is, they only contain clay bound water. Subsequently, we cure the as-dried samples in moist air for more than 24 h to obtain relatively dry samples with 2−3% water content and thus eliminate the damaging effect of the dehydration of clay minerals in the rock matrix. Then, we use the pumping pressure saturation method to completely saturate the samples for 48 h. We

Seismic rock-physics characteristics

Table 1 Physical properties, structural parameters of pores, and velocity data

Sample No.	Porosity (%)	Permeability (mD)	P-wave (km/s)	S-wave (km/s)	SS (mm^{-1})	Roundness	Average pore throat radius (μm)	Average aspect ratio
1	1.74	0.0082	5.29	3.07	35.65	0.88	12.1	0.045
2	2.01	0.0082	5.19	3.02	52.6	0.88	11.5	0.034
3	2.27	0.0159	5.47	3.16	35.97	0.87	13.7	0.043
4	1.82	0.0784	5.60	3.25	29.85	0.84	14.5	0.056
5	1.8	0.2473	6.04	3.52	20.23	0.91	18.5	0.091
6	1.78	0.0843	5.58	3.19	23.28	0.85	14.7	0.074
7	1.64	0.0149	5.77	3.28	24.55	0.87	15	0.069
8	0.99	0.0357	6.26	3.66	17.06	0.85	20.6	0.109
9	1.78	0.1062	5.70	3.29	20.94	0.85	13.8	0.103
10	1.22	0.1599	6.16	3.59	16.87	0.89	19.1	0.126
11	1.57	0.0681	6.56	3.74	15.2	0.81	26.8	0.136
12	2.14	0.0253	6.43	3.66	18.11	0.83	24.6	0.098
13	1.44	0.0873	6.20	3.55	17.18	0.83	20.8	0.123
14	1.81	0.1371	5.70	3.26	25.23	0.87	14	0.075
15	1.21	0.0462	5.54	3.25	26.65	0.89	14.3	0.075
16	2.14	0.0671	5.65	3.22	24.43	0.89	13.6	0.076
17	2.52	0.0671	5.51	3.18	25.51	0.87	14	0.069
18	1.18	0.0213	5.71	3.31	21.98	0.87	15.3	0.091
19	8.46	0.2551	5.46	3.16	26.84	0.86	12.9	0.073
20	1.99	0.0525	6.13	3.54	19.54	0.85	17.8	0.095
21	2.21	0.0145	6.07	3.55	19.1	0.87	17.5	0.097
22	1.96	0.1679	5.83	3.41	22.23	0.83	16.3	0.085
23	1.72	0.0109	5.29	3.06	37.93	0.89	11.1	0.044
24	2.89	0.0578	5.70	3.27	25.23	0.9	14.6	0.077
25	3.41	0.0322	5.18	3.03	44.46	0.84	11.1	0.037
26	2.01	0.0086	4.93	2.88	97.95	0.9	9.09	0.027
27	3.41	0.0082	4.58	2.68	281.19	0.85	7.25	0.02
28	1.5	0.0794	6.36	3.81	17.38	0.83	26.2	0.102
29	11.93	0.0258	4.29	2.53	32.31	0.89	16.1	0.056
30	4.18	0.0362	5.19	3.06	55.08	0.86	10.4	0.036
31	1.07	0.4436	5.79	3.41	21.33	0.84	14.9	0.078
32	0.75	0.0321	6.08	3.52	21.83	0.9	17.3	0.08
33	1.2	0.3873	5.82	3.48	23.71	0.87	15.6	0.077
34	1.57	0.0189	5.13	2.95	59.57	0.9	10.5	0.031
35	1.27	0.0810	5.55	3.3	27.48	0.88	13.7	0.064
36	2.56	0.0172	5.31	3.12	46.13	0.85	12.5	0.036
37	3.83	0.5041	4.62	3.11	239.88	0.94	6.1	0.022
38	2.88	0.0129	4.95	3.49	96.16	0.87	9.9	0.028
39	4.52	0.0598	5.42	2.88	29.1	0.81	14.5	0.061
40	4.72	0.0303	5.60	3.27	26.49	0.85	17.2	0.065

measured the porosity and permeability of the samples by the pulse-decay method and list the results in Table 1. Cylindrical specimens, 25.4 mm in diameter and 40–55 mm in height, were prepared and ground to less than 0.05 mm in the polishing slope of the two end surfaces. The velocity was measured by the ultrasonic pulse-echo method. The longitudinal and transversal wave frequency of the PZT transducer was 800 KHz and 350 KHz, respectively. During the experiment, the pressure was increased from 2 MPa to 60 MPa and measured every 2 MPa prior to 10 MPa and then once every 5 MPa. The time interval for every pressure point is 15 min to ensure pressure equilibration in the specimens. To measure the velocity under water-saturated conditions, we kept the pore pressure at 1 MPa for the nondraining conditions and the deviation of the confining and pore pressure to less than 0.3%. The time error of the oscilloscope is equal to or less than 0.01 μs; thus, the relative error of the longitudinal and transversal wave is correspondingly about 1% and 2%.

The P- and S-wave velocities of the samples under dry and water-saturated conditions increased with increasing confining pressure. The velocity–confining pressure relation is shown in Figure 2. We see that the P- and

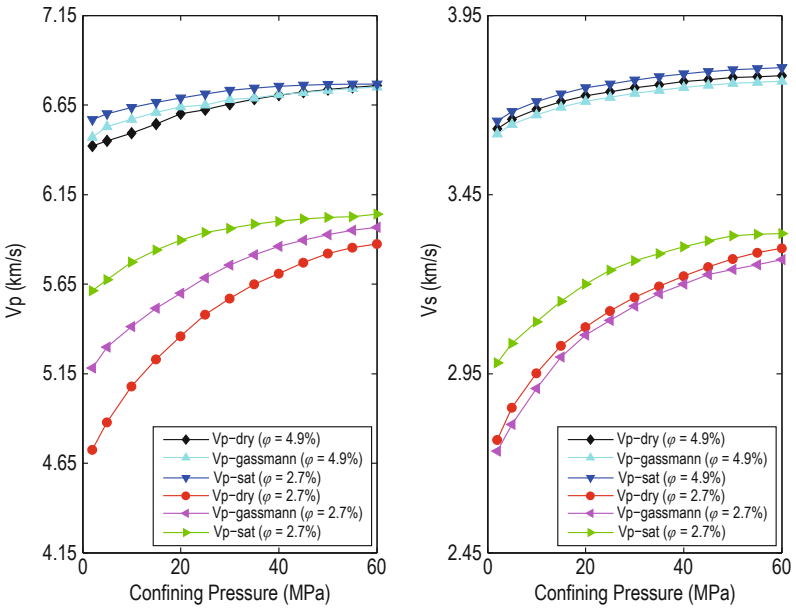

(a) P-wave velocity as a function of confining pressure

(b) S-wave velocity as a function of confining pressure

Fig.2 Variation of the P- and S-wave velocity of the carbonate rock samples under dry and saturated conditions.

S-wave velocities of specimens with porosity φ = 2.7% vary nonlinearly as a function of pressure (Figure 2a). Moreover, the P- and S-wave velocities increase rapidly when the pressure is less than 30 MPa, and change only slightly and nearly linearly with pressure higher than 30 MPa. Within the entire pressure range, the P- and S-wave velocities increased 24% and 20%, respectively, under dry conditions. For specimens with porosity φ = 4.9% (Figure 2b), we observe a nearly linear trend in the P- and S-wave velocities with increasing confining pressure and corresponding increases of 5.1% and 4%.

The observations suggest that the specimens contain microcracks that gradually close with increasing pressure and thus the longitudinal and transversal wave velocities increase, which reflects the double-pore structure of the rock samples. In addition, the rocks mainly contain rigid pores with large aspect ratio, such as dissolved pores, which reflects the single-pore structure of the rock samples.

Walsh (1956) expressed the relation between confining pressure and microcracks with the following equation

$$P_{close} = \left[\pi E_s / 4\left(1-v_s^2\right)\right]a_0 \approx E_s a_0, \qquad (1)$$

where P_{close} denotes the crack closure pressure, E_S is the Young's modulus of the rock matrix, v_s is the Poisson' s ratio of the rock matrix, and α_0 denotes the aspect ratio of the microcracks. For carbonates, the Young's modulus of the rock matrix is 84.3 GPa and the aspect ratio of microcracks is about 0.00036. Assuming that the length of the microcracks is about 3000 μm, the size of the corresponding microcracks or pore-throat radius is 0.001 mm, which is consistent with the magnitude of the microcracks in Figure 1. The P-wave velocity of water-saturated samples increased and the velocity increase was even more remarkable under low confining pressure. The experimental P-wave velocity is slightly higher than that predicted using the Gassmann equation. This suggests that the fluid-related velocity dispersion, such as squirt flow, also depends on the pore structure of the rock specimens. For samples with single-pore structure (φ = 4.9%), small differences in pore rigidity cause weak fluid-related velocity variability. In this case, the experimental results slightly differ from those predicted with the Gassmann equation. For samples with double-pore structural characteristics (φ = 2.7%), the apparent differences in the rigidity of pores apparently affect the fluid-related velocity dispersion because there are obvious differences between measurements and predictions based on Gassmann's equation. The differences decrease with increasing confining pressure, which reflects the increasing uniformity of the pores as the microcracks gradually close with increasing confining pressure. There is sample heterogeneity at the

Seismic rock-physics characteristics

pore or grain scale, which implies that mainly pore-scale squirt flow affects the dispersion of the P- and S-wave velocity of water saturated rock samples (Gurevich et al., 2009; Müller et al., 2010; Ba et al., 2011, 2013; Deng et al., 2012; Nie et al., 2012). The dispersion magnitude depends on the pore rigidity variations; furthermore, pore inhomogeneity contributes to the small pore-pressure discrepancies during seismic wave propagation. Pore-pressure equilibration is achieved within the half-period of the ultrasonic waves. The ultrasonic wave frequency can be thought as the low-frequency band of squirt flow and the ultrasonic measurements of water-saturated samples agree with the predictions based on Gassmann's equation. However, when the pore structure is strongly heterogeneous, the ultrasonic wave frequency is the high-frequency band of squirt flow, which leads to significant disagreement between measured and theoretically derived with Gassmann's equation data for water-saturated rock samples.

Figures 3a and 3b show the P- and S-wave velocities as a function of porosity under dry conditions. The P- and S-wave velocities decrease with increasing porosity; however, the data scatter is sufficiently strong and this does not allow establishing a velocity–porosity model. The P- and S-wave velocities range is 3.8 km/s −6.5 km/s and 2.4 km/s−3.7 km/s, respectively. At the same porosity, the P-wave velocity variation may exceed 1.5 km/s, whereas the S-wave velocity variation may exceed 0.8 km/s. The samples have the same mineral components; thus, the P- and S-wave velocity variations are attributed to differences in the pore types or structure at the same porosity (%). This also suggests that the type of pores in dense carbonate rocks affects the seismic elastic properties. Clearly, to characterize the seismic elastic properties of dense carbonate rocks, it is critical to construct simple but accurate models of the pore structure. Figure 3 also shows the results of calculations using the differential equivalent model (DEM). The aspect ratio of the pores was maintained constant, while the volume and the shear modulus of the samples was 76.8 GPa and 32 GPa, respectively. The measured velocity data in Figure 3 correspond to aspect ratio values between 0.01 and 0.99, and the single model value is presumably the average aspect ratio of the pores in the samples. Using the method of Xu and Payne (2009), we identified the primary pore types and structure of the samples. We assumed that the aspect ratio of the original intergranular pores is 0.2 and the velocity data for this aspect ratio indicate that the rocks contain more dissolved (casting) pores with large aspect ratio, whereas the microcracks, which have lower aspect ratios, gradually increase. The experimental results show that the velocities of most dry samples are below the model line for the 0.2 aspect ratio, which suggests the presence of microcracks.

Figure 3c shows the velocity ratio of P- and S-wave velocity vs P-wave velocity under dry conditions. The velocity ratio of dry samples varies between 1.78 and 1.88, and the correlation between the velocity ratio and P-wave velocity is positive. The above characteristics reflect how differences in microcracks affect the P- and S-wave velocities; the more microcracks a rock contains, the greater the reduction in P- and S-wave velocities is. The velocity reduction in P waves is higher than in S waves; hence, the velocity ratio decreases with increasing microcracks. We also observe weak negative correlation between porosity and velocity ratio, which suggests that dense carbonate rocks differ from regular pore-type carbonate rocks, namely, porosity does not affect the seismic elastic properties. Figure 3d shows the relation between sample porosity and permeability, with no significant correlation.

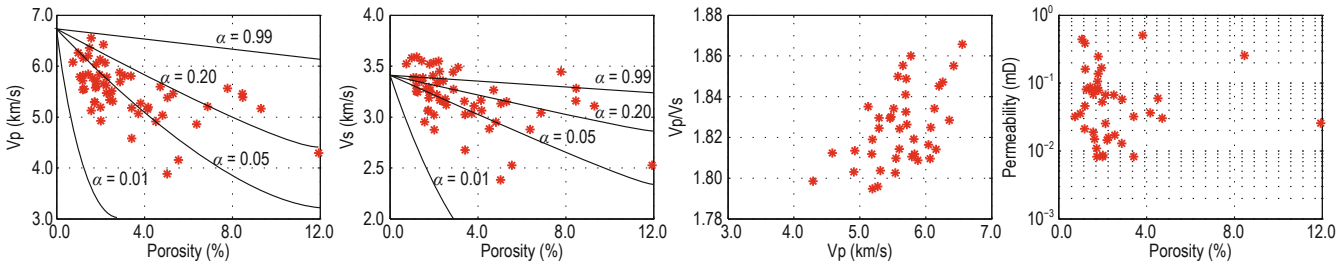

(a) P-wave velocity vs porosity (b) S-wave velocity vs porosity (c) P- and S-wave ratio vs P-wave velocity (d) permeability vs porosity

Fig.3 Rock-physics characteristics and physical properties of the carbonate samples.

The 41 samples of the Shanying formation have the following porosity and permeability characteristics. The maximum and minimum porosity is 11.8% and 0.58%, respectively, the porosity range is between 0.58% and 3.8%, and the average porosity is 2.48%. The maximum and minimum permeability is 0.504 mD and 0.0082 mD,

respectively, the permeability range is 0.01–0.15 mD, and the average permeability is 0.09 mD.

Figure 4 shows the specific surface and average pore-throat radius. The figure also shows the casting sheets of three representative samples. The color scale next to the right vertical axis corresponds to the P-wave velocity of the samples. From the casting sheets, we see that sample A is a dense micrite with mainly intergranular and intragranular dissolved pores. The SS and the average pore-throat radius is 17.4 mm^{-1} and 26.2 μm, respectively. Sample B is a dense sparry calcarenite with algae clumps cemented by sparry calcite, lacking well-developed primary intergranular pores, and mostly containing intergranular dissolved pores and microcracks. The SS and average pore-throat radius is 46.1 mm^{-1} and 12.5 μm, respectively. Sample C is a hydrocarbon-bearing dense micrite that lacks well-developed primary and dissolved pores, and mostly contains microcracks. The SS and average pore-throat radius is 239 mm^{-1} and 6.1 μm, respectively. The SS correlates with the average pore-throat radius negatively, which reflects the various combinations of the pore types in the samples: single dissolved (casting) pores, dissolved pores and microcracks, and microcracks. Pores become uniform with increasing pore-throat radius and the average pore-throat radius gradually decreases as the pores change from single dissolved (casting) pores → dissolved pores and microcracks → microcracks. In addition, the P- and S-wave velocities decrease with increasing SS and decreasing average pore-throat radius, which also suggests that the seismic elastic properties are controlled by the pore structure rather than porosity (%).

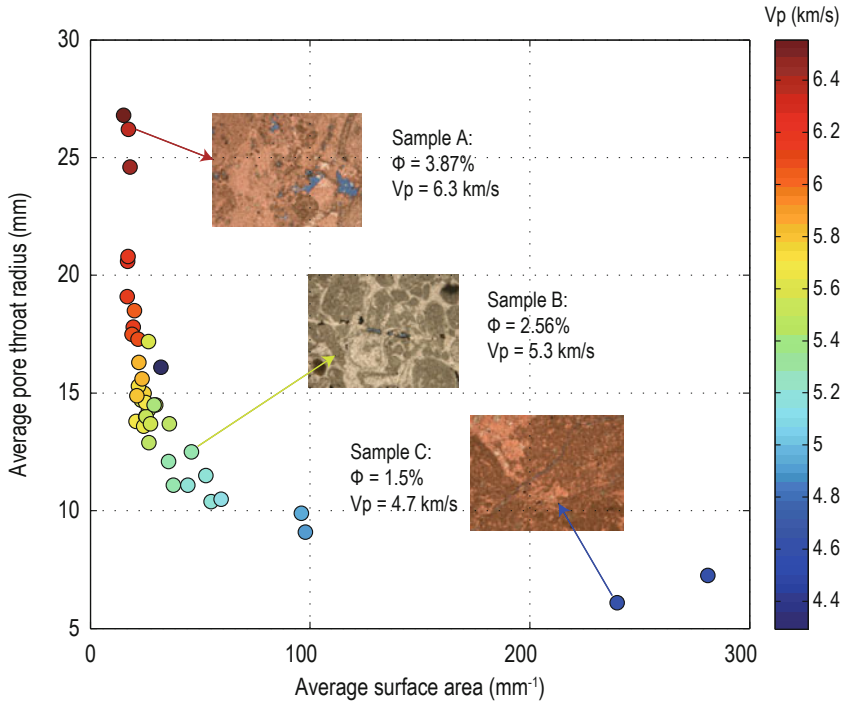

Fig.4 Average pore-throat radius vs specific surface of the carbonate rock samples.

To discuss the control of pore structure on the seismic elastic properties of dense carbonates, we considered the SS, average pore radius, pore roundness, and average aspect ratio along with the negatively correlated P-wave velocity and porosity in Figure 5. The data in Figure 5a suggest negative correlation between SS and P-wave velocity at the same porosity. The SS better reflects the variability in pore types and is especially high in samples with many microcracks. The high P-wave velocity rocks generally have SS less than 55 m^{-1}. Figure 5b shows that the average pore-throat radius and P-wave are positively correlated at the same porosity. The increase in the average pore-throat radius means that soft and hard pores become indistinguishable, which implies that soft pores decrease. High P-wave velocity samples have average pore-throat radius greater than 15 μm. Figure 5c shows the relation between pore roundness and P-wave velocity. The average roundness of the samples is greater than 0.8, indicating that the shape of the pores is nearly spherical and consistent with dissolved (casting) pores. There is no obvious relation between P-wave velocity and pore roundness because the wave velocity in dense

carbonates is strongly affected by the percentage of soft pores, represented by microcracks, whereas pore roundness describes the shape of dissolved (casting) pores. Figure 5d shows the linear relation between the average aspect ratio and P-wave velocity. The average aspect ratio variations mainly reflect the relative content of soft pores (microcracks) in the samples. If the content of microcracks is large, the average aspect ratio is small. The P-wave velocity is also directly affected by microcracks. The average aspect ratio of high P-wave velocity samples is generally greater than 0.07. Overall, high P-wave velocity carbonate samples correspond to low SS, high average pore-throat radius, and high average aspect ratio values.

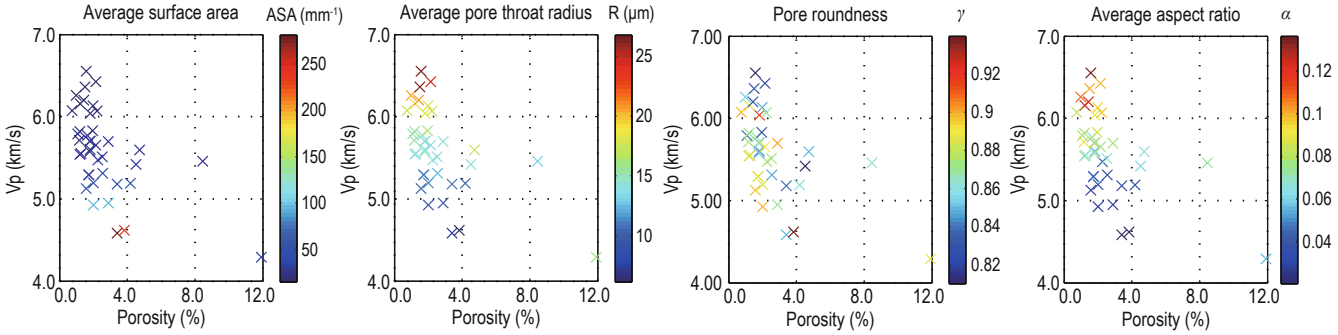

Fig.5 Pore-structure parameters and P-wave velocity.

Pore-structure characteristics also affect rock permeability. Figure 6 shows the relation between permeability and SS, and permeability and average aspect ratio at variable porosity (%). Samples with high permeability typically have low SS and high average aspect ratio. This is consistent with data calculated using the permeability equation of Kozeny. Note that samples with high SS and low average aspect ratio also have high permeability. High SS means that the microcracks in the samples have increased and consequently the permeability is high.

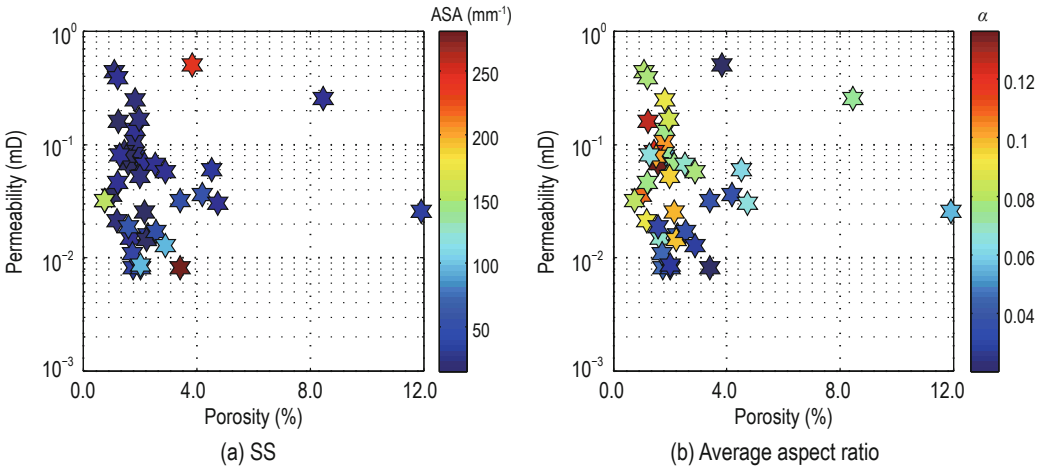

Fig.6 Relation between permeability and pore-structure parameters of the carbonate samples.

Differences in rock rigidity may affect the elastic waves and thus introduce fluid-related velocity dispersion and attenuation. In the laboratory, squirt flow is the primary fluid-related dispersion. Based on the above, we infer that high-velocity samples mainly include more dissolved (casting) pores, whereas low-velocity sample pores mainly include microcracks that have lower aspect ratios. Nevertheless, some samples have both types of pore structure. Pore types also affect the fluid-related velocity and thus water-saturated rock samples show differences in velocity. Figure 7 shows the residuals of the measured and calculated P-wave velocity as a function of SS and average aspect ratio. In the calculations, we used Gassmann's equation. There is no

strong linear relation between P-wave velocity residuals and SS. For SS less than 35 mm^{-1}, the pore types are mainly dissolved (casting) pores with high aspect ratios, which implies uniform pores. Thus, the rigidity of the pores is rather uniform and there is no basis for fluid-related velocity dispersion, such as squirt flow. Overall, the basic assumptions of Gassmann's equation are nearly satisfied, and ultrasonic data and predictions generally agree. For SS between 35 mm^{-1} and 150 mm^{-1}, the rocks mainly contain microcracks and are characterized by low aspect ratio and uniform pores, and show greater rigidity variation and less agreement between data and predictions. Similar variability is seen between the average aspect ratio and P-wave velocity residuals in Figure 7b. The pore structure of the samples is simple if the average aspect ratio is either high (> 0.10) or low (< 0.05). Consequently, there is no remarkable difference in pore rigidity and the fluid-related velocity dispersion is weak; hence, the P-wave residuals are small. If the average aspect ratio is neither high (> 0.10) nor low (< 0.05), dissolved (casting) pores with high rigidity and microcracks with low rigidity coexist. In this case, the differences in pore rigidity affect the P-wave velocity residuals.

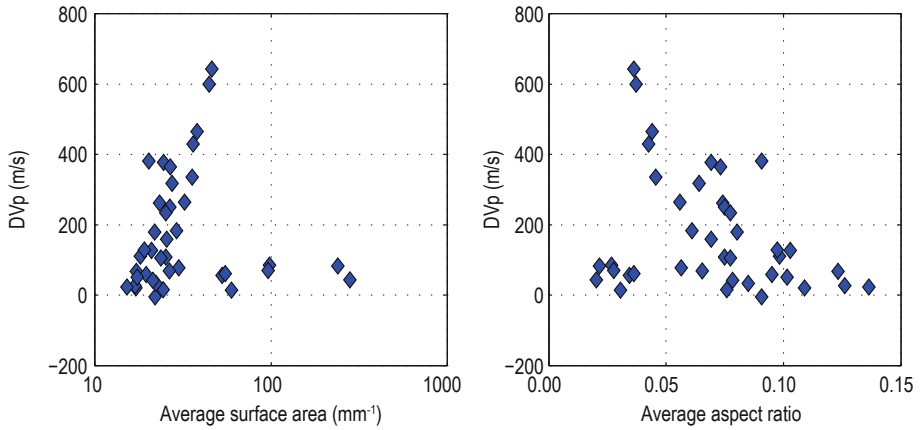

(a) residuals of measured and calculated P-wave velocity residuals vs SS

(b) residuals of measured and calculated P-wave velocity vs average aspect ratio

Fig.7 Effect of the pore structure of the carbonate samples on velocity.

Conclusions

Porosity (%) is not the primary controlling factor of the seismic elastic characteristics of dense carbonates. Pore-structure variability at the same porosity is more significant. In dense carbonate rock, the P- and S-wave velocity correlate with SS, average pore-throat radius, and average aspect ratio. High velocities correspond to low SS, high average pore-throat radius, and high average aspect ratio values. The pore structure of dense carbonate rocks also affects permeability; high-permeability samples have low SS and high average aspect ratio values.

Pore-structure variability in dense carbonate rocks affects the variability of fluid-related velocity data. For weak fluid-related velocity variability, ultrasonic data and predictions based on Gassmann's equation generally agree. For SS lower than 35 mm^{-1} and higher than 150 mm^{-1}, and average aspect ratio less than 0.05 and higher than 0.10 the agreement is good. For in-between SS and average aspect ratio values, the residuals between predicted and observed data vary significantly.

References

Agersborg, R., Johansen, T. A., Jakobsen, M., Sothcott, J., and Best, A., 2008, Effects of fluids and dual-pore systems on pressure-dependent velocities and attenuations in carbonates: Geophysics, **73**(5), N35–N47.

Anselmetti, F. S. and Eberli, G. P., 1993, Controls on sonic velocity in carbonates: Pure and Applied Geophysics, **141**, 287–323.

Anselmetti, F. S., and Eberli, G. P., 1999, The velocity-deviation log: A tool to predict pore type and permeability trends in carbonate drill holes from sonic and porosity or density logs: AAPG Bulletin, **83**, 450–466.

Ba, J., Carcinoe, J. M., and Nie, J. X., 2011, Biot-Rayleigh

theory of wave propagation in double-porosity media: Journal of Geophysical Research-solid earth, **116**, B06202.

Ba, J., Cao, H., Carcione, J. M., Tang, G., Yan, X. F., Sun, W. T., and Nie, J. X., 2013, Multiscale rock-physics templates for gas detection in carbonate reservoirs: Journal of Applied Geophysics, **93**, 77–82.

Baechle, G. T., Al-Kharusi, L., and Eberli, G. P., 2007, Effect of spherical pore shapes on acoustic properties: AAPG Annual Convention, Abstracts Volume, **16**, 7.

Baechle, G. T., Colpaert, A., Eberli, G. P., and Weger, R., 2008, Effects of microporosity on sonic velocity in carbonate rocks: The Leading Edge, **27**(8), 1012–1018.

Deng, J. X., Qu, S. L., and Wang, S. X., 2012, P-wave attenuation and dispersion in a porous medium permeated by aligned fractures–a new poroelastic approach: Journal of Geophysics and Engeerning, **9**(2), 115−26.

Gurevich, B., Makarynska, D., Paula, O., and Pervukhina, M., 2010, A simple model for squirt-flow dispersion and attenuation in fluid-saturated granular media: Geophysics, **75**, N109–N120.

Liu, S. G., Shan, Y. M., and Huang, S. J., 2006, Characteristics and variation pattern of acoustic parameters of carbonate reservoir rocks in Tahe oil field Tarim basin: Oil & Gas Geology, **27**(3), 399−404.

Müller, T. B., Gurevich, B., and Lebedev, M., 2010, Seismic wave attenuation and dispersion resulting from wave-induced flow in porous rocks—a review: Geophysics, **75**, 75A147–75A164.

Nie, J. X., Ba, J., Yang, D. H., Yan, X. F., Yuan, Z. Y. and Qiao, H. P., 2012, BISQ model based on a Kelvin-Voigt viscoelastic frame in a partially saturated porous medium: Applied Geophysics, **12**(2), 213–222.

Sharma, R., Prasad, M., Batzle, M., and Vega, S., 2013, Sensitivity of flow and elastic properties to fabric heterogeneity in carbonates: Geophysical Prospecting, **61**, 270–286.

Verwer, K., Eberli, G., Baechle, G., and Weger, R., 2010, Effect of carbonate pore structure on dynamic shear moduli: Geophysics, **75**(1), E1–E8.

Walsh, J. B., 1965, The effects of cracks on the compressibility of rock: Journal of Geophysical Researc h, **70**, 381−389.

Weger, R. J., Baechle, G. T., Masaferro, J. L., and Eberli, G. P., 2004, Effects of pore structure on sonic velocity in carbonates: 74th Ann. Internat. Mtg, Soc. Expl. Geophys.,, Expanded Abstracts, 1774.

Xu, S. Y. and Payne, M. A., 2009, Modeling elastic properties in carbonate rocks: The Leading Edge, **28**(2), 66–74.

Zhou, W. and Yang, H. X., 2006, Effects of fractures of rock on elastic property of rock and velocity-porosity relation: Oil Geophysical Prospecting, **40**(3), 334−338.

Pan Jian-Guo, senior geophysicist, obtained his B.S. in Exploration Geophysics from ChengDu University of Technology and his Ph.D. in petroleum geology from China University of Geosciences in 1983 and 2010, respectively. He is presently working in the Northwest Branch of RIPED. His research interests are petroleum exploration, the seismic properties of reservoirs, and rock physics.